Achievable Rate and Capacity Analysis for Ambient Backscatter Communications

Jing Qian, Yongxu Zhu, Chen He, Feifei Gao, and Shi Jin

***Abstract*—In this paper, we analyze the achievable rate for ambient backscatter communications under three different channels: the binary input and binary output (BIBO) channel, the binary input and signal output (BISO) channel, and the binary input and energy output (BIEO) channel. Instead of assuming Gaussian input distribution, the proposed study matches the practical ambient backscatter scenarios, where the input of the tag can only be binary. We derive the closed-form capacity expression as well as the capacity-achieving input distribution for the BIBO channel. To show the influence of the signal-to-noise ratio (SNR) on the capacity, a closed-form tight ceiling is also derived when SNR turns relatively large. For BISO and BIEO channel, we obtain the closed-form mutual information, while the semi-closed-form capacity value can be obtained via one dimensional searching. Simulations are provided to corroborate the theoretical studies. Interestingly, simulations show that: (i) the detection threshold maximizing the capacity of BIBO channel is the same as the one from the maximum likelihood signal detection; (ii) the maximal of the mutual information of all channels is achieved almost by a uniform input distribution; (iii) the mutual information of the BIEO channel is larger than that of the BIBO channel, but is smaller than that of the BISO channel.**

***Index Terms*—Ambient backscatter, capacity, mutual information, capacity-achieving input distribution.**

I. Introduction

THE Internet of Things (IoT) that could connect millions or even billions of physical objects (including typical ones such as computers and smartphones) to the Internet has drawn increasing attentions from both academia and industry recently [1]. However, as more and more things are being connected to IoT, how to power the huge number of devices without expensively using batteries has posed a significant challenge [2]. To enable ubiquitous communications between low-power devices, an innovative passive communication technique, called ambient backscatter, was presented in [3], [4]. Specifically, an information device utilizes ubiquitous radio frequency signals from ambient sources, such as TV broadcasting, cellular and Wi-Fi transmissions, as both the energy source and information carriers. This approach provides a promising solution for communications between batteryless devices and demonstrates its potentials in IoT.

Ambient backscatter communications make use of environmental wireless signals to harvest energy and transmit information, which gets rid of the battery and avoids heavy manual maintenance. The basic principles of ambient backscatter can be described as follows:

- The ambient source continuously offers service to its own legacy receivers, whose signalling can also be received by both the tag and the reader;
- The tag transmits binary symbols, bit 1 or bit 0, by backscattering or not backscattering the received ambient signals [5], respectively;
- The reader receives the signal from the ambient source and the backscattered signals from the tag, and can decode bits 1 and 0 with specific signal processing technologies.

Following [3], many signal detection techniques for ambient backscatter communications were designed. For example, the differential energy detection and joint energy detection were proposed in [6]–[8], respectively, where the transmitter employs the low rated differential on-off signaling. The authors of [9] considered the frequency selective channel and developed an ambient backscatter system over the orthogonal frequency division multiplexing (OFDM) modulated carriers. An interesting cooperative strategy was established in [10], where the receiver can decode the information not only from the transmitter but also from the ambient source. In addition, ambient backscatter is also applied into radio frequency powered cognitive radio networks to improve the performance of the secondary systems [11]. Moreover, authors of [12] designed a Manchester code based ambient backscattering strategy in order to remove the necessity of estimating the decision threshold, and to enable immediate symbol-by-symbol detection.

Compared with the active radio protocols such as Bluetooth, ZigBee, and Wi-Fi, the operating data rate of the ambient backscatter system was relatively limited. Some methods were designed to enhance the data rates through the use of multi-antenna processing [4], where up to 1 Mbps can be

This work was supported in part by the National Natural Science Foundation of China under Grant 61531011, 61831013, 61771274, by the National Major Project under Grant 2016ZX03001023-003, by the Beijing Municipal Natural Science Foundation under Grant 4182030, L182042, and the R&D Project of the Science, Technology and Innovation Commission of Shenzhen Municipality No. JCYJ20180306170617062. The work of C. He was supported by National Natural Science Foundation of China under Grant 61701401. *(Corresponding author: Feifei Gao.)*

J. Qian is with Department of Automation, Tsinghua University, Beijing 100084, P.R. China (Email: qian-j13@tsinghua.org.cn).

Y. Zhu is with the Department of Electrical and Manufacturing Engineering, Loughborough University, U.K. (Email: y.zhu4@lboro.ac.uk).

C. He is with School of Information Science and Technology, Northwest University, Xi'An, Shanxi 710127, P.R. China (Email: chenhe@nwu.edu.cn).

F. Gao is with Beijing National Research Center for Information Science and Technology (BNRist), Department of Automation, Tsinghua University, Beijing 100084, P.R. China, and is also with Key Laboratory of Digital TV System of Guangdong Province and Shenzhen City, Research Institute of Tsinghua University in Shenzhen, Shenzhen 518057, P.R. China (e-mail: feifeigao@ieee.org).

S. Jin is with the National Communications Research Laboratory, Southeast University, Nanjing 210096, P.R. China (Email: jinshi@seu.edu.cn).

achieved at the cost of receiver size and complexity. In term of achievable date rate analysis, the existing works assume Gaussian input and directly apply the Shannon theorem [13] to evaluate typical information-theoretic figures of merit for both the ambient source and backscatter systems. However, such assumption is far from the practical binary signalling in the ambient backscatter system.

In this paper, we consider three different types of channels for ambient backscatter communications and analyze their corresponding achievable rate as well as the capacity. Firstly, we study the binary input and binary output (BIBO) channel from an information-theoretic point of view[1], where the input of the channel is the on-off keying state at the tag. The output of the channel is obtained from an energy detector [15] at the reader, where the received continuous signals are converted into discrete binary symbols. Similar to [16], [17], we here treat the energy detector as a part of the channel during the capacity analysis, and then compute the capacity-achieving input distribution of the BIBO channel. To show the influence of signal-to-noise ratio (SNR) on the capacity, we also derive the closed-form tight capacity ceiling when the SNR of the source goes relatively large. Secondly, we consider the binary input and signal output (BISO) channel, where the output of the channel is exactly the continuous signal received at the reader. Since the energy of the received signal is the key information-bearing statistics [18] during the detection, we, lastly, treat the energy computator as a continuous communication channel and look into the binary input and energy output (BIEO) channel, where the output of the channel is the energy of the continuous signals received at the reader. We derive the closed-form expressions of the mutual information of the BISO and BIEO channels, respectively, and obtain the impact of the partition number for the Riemann Integral on their mutual information. Semi-closed-form values of the capacities can then be obtained from one dimensional searching. Interestingly, simulations show that (i) for the BIBO channel, the threshold maximizing the capacity is the same as the one obtained from the maximum likelihood (ML) detector; (ii) for all three types of channels, the maximum values of the mutual information are almost achieved by a uniform distribution for the input; (iii) the mutual information of BIEO channel is larger than that of the BIBO channel, but is smaller than that of the BISO channel.

The underlying differences between the developed rate analysis for ambient backscatter communications and that for conventional active system lie in the following two aspects: 1) The information signal is carried on an unknown ambient signal, which formulate a completely different analysis approach. Moreover, the unknown ambient radio also acts as an interference and the enhance the difficulty of the analysis; 2) Gaussian input distribution is normally used in an active system because it could provide a better approximation for high order constellations. However, Gaussian input distribution would not be a suitable one for the low-power binary ambient backscatter, and hence the developed rate analysis would be much different and difficult than that for the active system.

[1]Some of our preliminary results were published in [14].

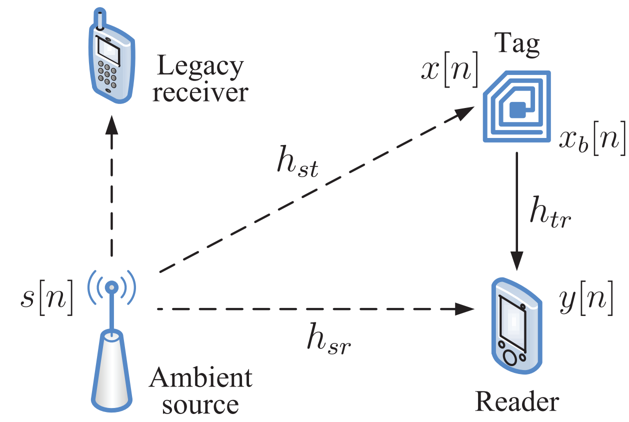

Fig. 1. System model for ambient backscatter communications.

The rest of this paper is organized as follows. Section II briefly reviews the system model and the corresponding detection method. Section III derives the mutual information of the BIBO channel, as well as the capacity and the capacity-achieving input distribution. The mutual information of the BISO channel and the BIEO channel are derived in Section IV and Section V, respectively. Simulations are then provided to corroborate the proposed studies in Section VI. Finally, Section VII concludes the paper.

Notations: Vectors are boldfaced letters: $\|\boldsymbol{y}\|$ denotes the Euclidean norm of vector $\boldsymbol{y}$. Scalars are lowercase letters: $|h|$, $\Re\{h\}$ and $\Im\{h\}$ denotes the modulus, real part and imaginary part of complex number h, respectively. Random variables (RVs) are uppercase letters: the statistic expectation and s-tatistic variance of RV X are denoted as $\mathbb{E}\{X\}$ and $\mathbb{D}\{X\}$, respectively; $\{X_k\}$ denotes a sequence of RVs. $\mathcal{N}(\mu, \sigma^2)$ and $\mathcal{CN}(\mu, \sigma^2)$ represent the Gaussian distribution and complex Gaussian distribution with mean μ and variance σ^2, respectively; in particular, a complex Gaussian RV $X \sim \mathcal{CN}(0, \sigma^2)$ with independent and identically distributed zero-mean Gaussian real and imaginary components is circularly symmetric, i.e., $\Re\{X\}, \Im\{X\} \sim \mathcal{N}(0, \sigma^2/2)$.

II. Problem Formulation

A. System Model

Consider a typical ambient backscatter communication system that consists of an ambient source, a batteryless tag and a reader, as illustrated in Fig.1. Denote h_{st}, h_{sr} and h_{tr} as the channel coefficients between the source and the reader, between the source and the tag, and between the tag and the reader, respectively.

When the ambient source serves its own legacy receivers, tag could also receive signals as

$$x[n] = h_{st} s[n], \tag{1}$$

where $s[n]$ is the unknown signal from the ambient source and is generally assumed to be circularly symmetric complex Gaussian distribution, i.e., $s[n] \sim \mathcal{CN}(0, P_s)$.

Part of the ambient signal $x[n]$ will be harvested to support the circuit of the tag, while the others will be backscattered or non-backscattered to realize the "1", "0" transmission.

Normally the IoT tag transmits data at a much lower rate than the legacy signal, and we can assume tag's symbol remains unchanged for N (an even number without loss of generality) consecutive $s[n]$'s. Denote the binary transmitter symbols of the tag as $d \in \{0, 1\}$. Then the signal backscattered by the tag is

$$x_b[n] = \alpha d x[n], \quad n = 1, \cdots, N, \tag{2}$$

where α is a coefficient representing the scattering efficiency and antenna gain. Since the tag circuit consists only of passive components and takes few signal processing operations, its thermal noise is usually negligible [19].

As the reader obtains the superposition of the signal from the ambient source and the modulated signal backscattered from the tag, the received signal $y[n]$ is expressed as

$$y[n] = (h_{sr} + \alpha h_{st} h_{tr} d) s[n] + w[n], \tag{3}$$

where $w[n]$ is the zero-mean additive white Gaussian noise with noise power N_w, i.e., $w[n] \sim \mathcal{CN}(0, N_w)$. We then formulate a received vector corresponding to the tag's symbol d as $\boldsymbol{y} = [y[1], \cdots, y[N]]^T$.

B. Maximum Likelihood Detection

Let us now describe how the reader decodes the tag's information d. Denote $h_0 = h_{sr}$ and $h_1 = h_{sr} + \alpha h_{st} h_{tr}$. There is

$$y[n] = \begin{cases} h_0 s[n] + w[n] \sim \mathcal{CN}(0, \sigma_0^2), & d = 0, \\ h_1 s[n] + w[n] \sim \mathcal{CN}(0, \sigma_1^2), & d = 1, \end{cases} \tag{4}$$

with variances

$$\sigma_0^2 \triangleq |h_0|^2 P_s + N_w, \quad \sigma_1^2 \triangleq |h_1|^2 P_s + N_w. \tag{5}$$

Denote $\mathcal{H}_i$ as the hypothesis that $d = i$ is transmitted by the tag. For the optimal ML detection [15], the likelihood ratio is

$$\Lambda(\boldsymbol{y}) = \frac{p(\boldsymbol{y}|\mathcal{H}_0)}{p(\boldsymbol{y}|\mathcal{H}_1)} = \frac{\sigma_1^{2N}}{\sigma_0^{2N}} \exp\left(\frac{\sigma_0^2 - \sigma_1^2}{\sigma_0^2 \sigma_1^2} z\right), \tag{6}$$

where $z = \sum_{n=1}^{N} |y[n]|^2$ is the received signal energy. Then the ML detection can be simplified to

$$\Lambda(\boldsymbol{y}) \underset{\mathcal{H}_1}{\overset{\mathcal{H}_0}{\gtrless}} 1 \Leftrightarrow \begin{cases} z \underset{\mathcal{H}_1}{\overset{\mathcal{H}_0}{\gtrless}} T_{\mathrm{ML}}, & \sigma_0^2 > \sigma_1^2, \\ z \underset{\mathcal{H}_1}{\overset{\mathcal{H}_0}{\lessgtr}} T_{\mathrm{ML}}, & \sigma_0^2 < \sigma_1^2, \end{cases} \tag{7}$$

which is exactly the energy detection and

$$T_{\mathrm{ML}} = \frac{N \sigma_0^2 \sigma_1^2}{\sigma_0^2 - \sigma_1^2} \ln \frac{\sigma_0^2}{\sigma_1^2} \tag{8}$$

is the optimal detection threshold.

C. Information Theory Background

To match the practical ambient backscattering scenario, we mainly focus on the binary input case [20], where the tag input is denoted as D whose possible values are $d = 0$ or $d = 1$. Clearly, the Shannon's capacity formula with Gaussian input should not be applied for (3) to derive the capacity for ambient backscatter system.

Case 1: If the channel output is a binary discrete random variable, denoted as $\hat{D}$ whose possible values are $\hat{d} = 0$ or $\hat{d} = 1$, then the channel is defined as the BIBO channel. The input probability distribution of the channel is denoted as $\boldsymbol{p} = [P(d = 0), P(d = 1)]$. Given the input $d = i$, the conditional probability of having the output $\hat{d} = j$ is $P(\hat{d} = j | d = i)$. For the BIBO channel with input D and output $\hat{D}$, the mutual information can be expressed as

$$I(D; \hat{D}) = \sum_{i=0,1} P(d = i) I(d = i; \hat{D}) \tag{9}$$

where $I(d = i; \hat{D})$ is the average mutual information between the input d_i and the output $\hat{D}$, and is given by[2]

$$I(d = i; \hat{D}) = \sum_{j=0}^{1} P(\hat{d}=j|d=i) \log \frac{P(\hat{d}=j|d=i)}{\sum\limits_{k=0}^{1} P(d=k) P(\hat{d}=j|d=k)}. \tag{10}$$

Case 2: If the channel output is a continuous random variable, denoted as Y whose value ranges from $-\infty$ to $+\infty$, then the channel is defined as the binary input and continuous output channel. Given the input $d = i$, the conditional probability function of having output y is $f(y|d = i)$. For the binary discrete input D and continuous output Y, the mutual information can be expressed as [21]

$$I(D; Y) = \sum_{i=0,1} P(d = i) I(d = i; Y), \tag{11}$$

where

$$I(d=i; Y) = \int_{-\infty}^{\infty} f(y|d=i) \log \frac{f(y|d=i)}{\sum\limits_{k=0}^{1} P(d=k) f(y|d=k)} \mathrm{d}y. \tag{12}$$

III. Binary Input and Binary Output Channel

From Section II.B we know that the optimal detection is to pass the received signal to an energy detector and then yield the binary output "0" and "1". Considering together the binary input, we could then imagine the whole transmission from the binary input to binary output as a BIBO channel, as shown in Fig. 2, where the energy detector with an uncertain threshold T_h (not necessarily T_{ML}) can be treated as a part of the ambient backscatter channel [17].

Let us denote the input alphabet and the output alphabet as $D = \{0, 1\}$ and $\hat{D} = \{0, 1\}$, respectively. Define the binary input distribution as $P(d = 0) = p$, $P(d = 1) = 1 - p$ and denote $\boldsymbol{p} = [p, 1 - p]$. Meanwhile, define the binary output

[2] Throughout the paper, $\log x$ stands for log base 2 of x.

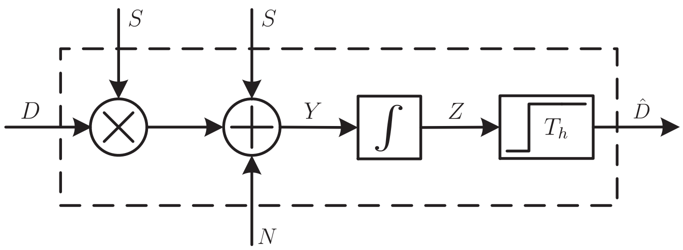

Fig. 2. The BIBO channel: the binary input D is subject to the ambient source signal S and the addictive noise N, and the received signal energy is quantized with threshold T_h to yield the binary output $\hat{D}$.

distribution as $P(\hat{d}=0)=q$, $P(\hat{d}=1)=1-q$ and denote $\boldsymbol{q}=[q,1-q]$. The transition probability matrix $\boldsymbol{P}$ of the system is

$$\boldsymbol{P}=\begin{pmatrix} P_{0|0} & P_{1|0} \\ P_{0|1} & P_{1|1} \end{pmatrix}=\begin{pmatrix} P_{0|0} & 1-P_{0|0} \\ P_{0|1} & 1-P_{0|1} \end{pmatrix}, \quad (13)$$

where $P_{j|i}$ denotes the conditional probability of getting the output j given the input i.

Due to symmetry, we only study the case where $\sigma_0^2>\sigma_1^2$ while that of $\sigma_0^2<\sigma_1^2$ can be similarly obtained. In this case, there is

$$P_{0|i}=\Pr(z>T_h|\mathcal{H}_i)=\int_{T_h}^{\infty} f(z|\mathcal{H}_i)\mathrm{d}z, \quad (14)$$

where $f(z|\mathcal{H}_i)$ is the probability density function (PDF) of z under hypothesis $\mathcal{H}_i$. Since z is a central chi-square random variable with $2N$ degrees of freedom (DOF), $f(z|\mathcal{H}_i)$ can be computed as

$$f(z|\mathcal{H}_i)=\frac{z^{N-1}\mathrm{e}^{-\frac{z}{\sigma_i^2}}}{\Gamma(N)\sigma_i^{2N}}. \quad (15)$$

Thus, $P_{0|i}$ is obtained by substituting $f(z|\mathcal{H}_i)$ into (14) as

$$P_{0|i}=\frac{\Gamma\left(N,\frac{T_h}{\sigma_i^2}\right)}{\Gamma(N)}. \quad (16)$$

where $\Gamma(N,x)$ denotes the upper incomplete Gamma function

$$\Gamma(N,x)=\int_x^{\infty} t^{N-1}\mathrm{e}^{-t}\mathrm{d}t. \quad (17)$$

A. Mutual Information

It can be readily obtained from the law of total probability that

$$q=pP_{0|0}+(1-p)P_{0|1}. \quad (18)$$

Let $h(p)$ be the binary entropy function:

$$h(p)\triangleq -p\log p-(1-p)\log(1-p). \quad (19)$$

Then the mutual information between input D and output $\hat{D}$ can be written as

$$\begin{aligned} I(D;\hat{D}) &= H(\hat{D})-H(\hat{D}|D) \\ &= h(q)-[ph(P_{0|0})+(1-p)h(P_{0|1})]. \end{aligned} \quad (20)$$

B. Capacity-achieving Input Distribution

We see that the mutual information (20) is the function only of $\boldsymbol{p}$, and we then define $I(D;\hat{D})=I(\boldsymbol{p})$. According to the definition, the channel capacity is

$$C=\max_{\boldsymbol{p}} \ I(\boldsymbol{p}). \quad (21)$$

Lemma 1. The necessary and sufficient condition on the input distribution $\boldsymbol{p}^*=[p^*,1-p^*]$ to achieve capacity is [22]:

If there exists some scalar $E>0$ such that

$$I(d=0;\hat{D})|_{\boldsymbol{p}=\boldsymbol{p}^*}=I(d=1;\hat{D})|_{\boldsymbol{p}=\boldsymbol{p}^*}=E, \quad (22)$$

where $I(d=i;\hat{D})$ is the mutual information for input $d=i$ averaged over the output, then the value of E is exactly the channel capacity.

Theorem 1. For the BIBO channel of ambient backscatter, the capacity-achieving input distribution is

$$p^*=\frac{q^*-P_{0|1}}{P_{0|0}-P_{0|1}}, \quad (23)$$

where

$$q^*=\frac{1}{1+2^{d(P_{0|0},P_{0|1})}} \quad (24)$$

is the corresponding output distribution and $d(P_{0|0},P_{0|1})\triangleq\frac{h(P_{0|0})-h(P_{0|1})}{P_{0|0}-P_{0|1}}$.

Proof: The mutual information for input $d=i$ averaged over output can be expressed as

$$\begin{aligned} I(d=i;\hat{D}) &= \sum_{j=0,1} P_{j|i}\log\frac{P_{j|i}}{\sum_{k=0,1} P(d=k)P_{j|k}} \\ &= P_{0|k}\log\frac{P_{0|k}}{q}+(1-P_{0|k})\log\frac{1-P_{0|k}}{1-q} \\ &= -h(P_{0|k})+P_{0|k}\log\frac{1-q}{q}-\log(1-q), \end{aligned} \quad (25)$$

where $h'(q)=\log\frac{1-q}{q}$ is obtained from the derivative of $h(q)$.

From Lemma 1, we know the capacity-achieving output distribution $\boldsymbol{q}^*=[q^*,1-q^*]$ can be obtained from $I(d=0;\hat{D})=I(d=1;\hat{D})$ as (24). Moreover, the capacity-achieving input distribution p^* can be computed from (18) as (23). ■

Therefore, for the BIBO channel of ambient backscatter, the closed-form capacity is given by

$$C_{\mathrm{BIBO}}=-h(P_{0|0})+P_{0|0}h'(q^*)-\log(1-q^*). \quad (26)$$

C. Optimal Threshold for Capacity

Similar to [23], the capacity of BIBO channel is a function of the threshold T_h. In this subsection, we will derive the optimal T_h that maximizes (26).

We can obtain from (26) that

$$\begin{aligned} C_{\mathrm{BIBO}}(T_h)\triangleq &-h(P_{0|0})+(P_{0|0}-1)d(P_{0|0},P_{0|1}) \\ &+\log\left(1+2^{d(P_{0|0},P_{0|1})}\right). \end{aligned} \quad (27)$$

Then the optimal threshold can be obtained from the following optimization problem

$$T_h^* = \arg\max \ C_{\text{BIBO}}(T_h). \tag{28}$$

The derivative of (27) is computed as follows

$$\frac{\partial C_{\text{BIBO}}(T_h)}{\partial T_h} = \left[d(P_{0|0}, P_{0|1}) - h'(P_{0|0})\right] \frac{\partial P_{0|0}}{\partial T_h} + \left[P_{0|0} - \frac{1}{1+2^{d(P_{0|0},P_{0|1})}}\right] \frac{\partial d(P_{0|0}, P_{0|1})}{\partial T_h}, \tag{29}$$

where

$$\frac{\partial d(P_{0|0}, P_{0|1})}{\partial T_h} = \frac{1}{P_{0|0} - P_{0|1}} \left[h'(P_{0|0})\frac{\partial P_{0|0}}{\partial T_h} - h'(P_{0|1})\frac{\partial P_{0|1}}{\partial T_h} - d(P_{0|0}, P_{0|1}) \left(\frac{\partial P_{0|0}}{\partial T_h} - \frac{\partial P_{0|1}}{\partial T_h}\right)\right]. \tag{30}$$

From (16) and (17), we have

$$\frac{\partial P_{0|i}}{\partial T_h} = \frac{T^{N-1} \mathrm{e}^{-\frac{T_h}{\sigma_i^2}}}{\Gamma(N)\sigma_i^{2N}}. \tag{31}$$

The optimal threshold should be achieved when $\frac{\partial C_{\text{BIBO}}(T_h)}{\partial T_h} = 0$ holds whose closed-form expression is, unfortunately, hard to obtain. Nevertheless, since $C_{\text{BIBO}}(T_h)$ is a function of one single variable, we could simply apply a one-dimensional searching in $\frac{\partial C_{\text{BIBO}}(T_h)}{\partial T_h} = 0$ to obtain the optimal threshold at certain SNR value. Interestingly, it will be shown in the later simulation that T_h^* is almost the same as T_{ML} for various channel realizations.

D. Capacity Ceiling

It has been shown in [15] that the symbol detection in ambient backscatter communications will meet an error floor when SNR goes to infinity. Correspondingly, the capacity is also expected to meet an upper bound when SNR goes to infinity, referred to as the capacity ceiling. Since we do not have a closed form T_h^*, we here adopt the alternative threshold T_{ML} to illustrate the effect of the capacity ceiling. Nevertheless, it will be shown in the later simulations that T_{ML} almost provide the same capacity value as T_h^*.

For ambient backscatter communications, N is generally large and thus the following approximation holds [24]

$$\frac{\Gamma(N, x)}{\Gamma(N)} \approx Q\left(\frac{x}{\sqrt{N}} - \sqrt{N}\right). \tag{32}$$

With T_{ML} and (32), $P_{0|i}$ can be approximated by

$$P_{0|i} \approx Q\left(\sqrt{N}\left[\frac{|h_{\bar{i}}|^2 + 1/\gamma}{|h_0|^2 - |h_1|^2} \ln\left(\frac{|h_0|^2 + 1/\gamma}{|h_1|^2 + 1/\gamma}\right) - 1\right]\right) \triangleq Q\left(\sqrt{N}\left[\frac{g_i(\gamma)}{|h_0|^2 - |h_1|^2} - 1\right]\right), \tag{33}$$

where $\bar{i} = 1 \oplus i$, $\gamma = P_s/N_w$ denotes SNR of the ambient source, and $g_i(\gamma)$ is defined as the corresponding item.

From the fact that

$$Q(x) = \int_x^{+\infty} \frac{1}{\sqrt{2\pi}} \exp\left(-\frac{1}{2}t^2\right) \mathrm{d}t, \tag{34}$$

the derivative of $P_{0|i}$ with respective to γ is computed as

$$\frac{\partial P_{0|i}}{\partial \gamma} = \frac{-\sqrt{N} \exp\left(-\frac{N\left(\frac{g_i(\gamma)}{|h_0|^2 - |h_1|^2} - 1\right)^2}{2}\right)}{\sqrt{2\pi}(|h_0|^2 - |h_1|^2)} \frac{\partial g_i(\gamma)}{\partial \gamma}. \tag{35}$$

For $\sigma_0^2 > \sigma_1^2$, i.e., $|h_0|^2 > |h_1|^2$, there is

$$\frac{\partial g_i(\gamma)}{\partial \gamma} = \frac{1}{\gamma^2}\left[\frac{|h_0|^2 - |h_1|^2}{|h_i|^2 + \frac{1}{\gamma}} - \ln\left(1 + \frac{|h_0|^2 - |h_1|^2}{|h_1|^2 + \frac{1}{\gamma}}\right)\right]. \tag{36}$$

Since

$$\frac{\partial g_0(\gamma)}{\partial \gamma} = \frac{1}{\gamma^2}\left[1 - \frac{|h_1|^2 + \frac{1}{\gamma}}{|h_0|^2 + \frac{1}{\gamma}} + \ln\left(\frac{|h_1|^2 + \frac{1}{\gamma}}{|h_0|^2 + \frac{1}{\gamma}}\right)\right], \tag{37}$$

and $x - 1 > \ln x$ for $x > 0$, we obtain $\frac{\partial g_0(\gamma)}{\partial \gamma} < 0$; Meanwhile, since $x > \ln(1+x)$ for $x > 0$, we have $\frac{\partial g_1(\gamma)}{\partial \gamma} > 0$. Thus, $P_{0|0}$ and $P_{0|1}$ are increasing and decreasing functions of γ, respectively. Moreover, it can be checked that when γ turns to infinity, $P_{0|0}$ and $P_{0|1}$ will respectively meet a ceiling and a floor at

$$P_{0|0}^{\text{ce}} \triangleq Q\left(\sqrt{N}\left[\frac{|h_1|^2}{|h_0|^2 - |h_1|^2} \ln\left(\frac{|h_0|^2}{|h_1|^2}\right) - 1\right]\right), \tag{38}$$

$$P_{0|1}^{\text{fl}} \triangleq Q\left(\sqrt{N}\left[\frac{|h_0|^2}{|h_0|^2 - |h_1|^2} \ln\left(\frac{|h_0|^2}{|h_1|^2}\right) - 1\right]\right). \tag{39}$$

Substituting (38) and (39) into (26), we know the channel capacity will reach a ceiling at

$$C_{\text{BIBO}}^{\text{ce}} \triangleq -h(P_{0|0}^{\text{ce}}) + P_{0|0}^{\text{ce}} h'(\bar{q}) - \log(1 - \bar{q}), \tag{40}$$

when γ becomes large, where

$$\bar{q} = \frac{1}{1 + 2^{\frac{h\left(P_{0|0}^{\text{ce}}\right) - h\left(P_{0|1}^{\text{fl}}\right)}{P_{0|0}^{\text{ce}} - P_{0|1}^{\text{fl}}}}}. \tag{41}$$

E. Binary Symmetric Channel

It is also of interest to see when would the BIBO channel become a binary symmetric channel (BSC), i.e., the errors are symmetric $P_{0|1} = P_{1|0}$, by setting a proper detection threshold T_h. Let us first write the energy detection rule of BSC as

$$\begin{cases} z \underset{\mathcal{H}_1}{\overset{\mathcal{H}_0}{\gtrless}} T_{\text{BSC}}, & \sigma_0^2 > \sigma_1^2, \\ z \underset{\mathcal{H}_1}{\overset{\mathcal{H}_0}{\lessgtr}} T_{\text{BSC}}, & \sigma_0^2 < \sigma_1^2. \end{cases} \tag{42}$$

For a relatively large N, z can be well approximated by Gaussian distribution as

$$f(z|\mathcal{H}_i) = \frac{1}{\sqrt{2\pi N \sigma_i^4}} \exp\left[-\frac{\left(z - N\sigma_i^2\right)^2}{2N\sigma_i^4}\right]. \tag{43}$$

For case $\sigma_0^2 > \sigma_1^2$, $P_{0|1}$ and $P_{1|0}$ can be expressed as

$$P_{0|1} = \int_{T_{\text{BSC}}}^{\infty} f(z|\mathcal{H}_1)\mathrm{d}z = Q\left(\frac{T_{\text{BSC}} - N\sigma_1^2}{\sqrt{N}\sigma_1^2}\right),$$
$$P_{1|0} = \int_{-\infty}^{T_{\text{BSC}}} f(z|\mathcal{H}_0)\mathrm{d}z = 1 - Q\left(\frac{T_{\text{BSC}} - N\sigma_0^2}{\sqrt{N}\sigma_0^2}\right). \tag{44}$$

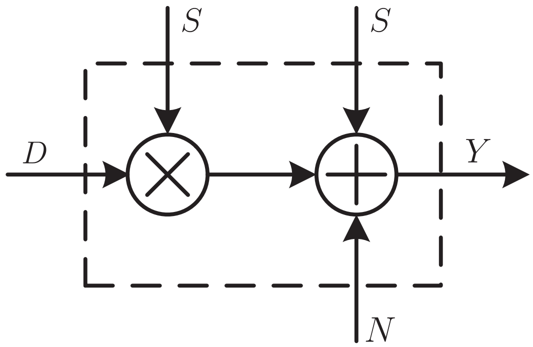

Fig. 3. Illustration of BISO channel

It can be easily computed from $P_{0|1} = P_{1|0}$ that

$$T_{\rm BSC} = \frac{2N\sigma_0^2\sigma_1^2}{\sigma_0^2+\sigma_1^2} \tag{45}$$

is the threshold to get the BSC. Similarly, for case $\sigma_0^2 < \sigma_1^2$, the threshold to get the BSC is also calculated as (45). Hence, the BSC has the capacity

$$C_{\rm BSC} = 1 - h(P_{0|1}), \tag{46}$$

which is a specific expression of the general one (26) when $P_{0|1} = P_{1|0}$.

IV. Binary Input and Signal Output Channel

From the information theoretical viewpoint, signal processing such as detecting with a threshold at the receiver would artificially cause information loss. Hence, another interest of research is to find out how much the information can be transmit from the tag to the receiver without any artificial loss. Hence, in this section we consider continuous signal received at the reader as the channel output, i.e., BISO channel, as depicted in Fig. 3.

The BISO channel is consisted of the discrete input $D = \{d = 0, d = 1\}$, the continuous output Y and a set of PDFs $f(y|d = i)$ describing the relationship between D and Y.

Based on the assumption that $s[n] \sim \mathcal{CN}(0, P_s)$, the signal received at the reader, Y, follows the circularly symmetric complex Gaussian distribution for given input $d = i$. Denote $Y \sim \mathcal{CN}(0, \sigma_i^2)$. Let $Y_{\rm R} = \Re\{Y\}$ and $Y_{\rm I} = \Im\{Y\}$. It can be readily found that $Y_{\rm R}$ and $Y_{\rm I}$ are independent from each other, and they both follow the Gaussian distribution, i.e., $Y_{\rm R}, Y_{\rm I} \sim \mathcal{N}(0, \frac{\sigma_i^2}{2})$. Thus we have

$$f(y_{\rm R}|d=i) = \frac{1}{\sqrt{\pi\sigma_i^2}} {\rm e}^{-\frac{y_{\rm R}^2}{\sigma_i^2}}, \tag{47}$$

and

$$I(D;Y) = I(D;Y_{\rm R}) + I(D;Y_{\rm I}) = 2I(D;Y_{\rm R}). \tag{48}$$

According to (11), the mutual information between D and $Y_{\rm R}$ can be computed as

$$I(D;Y_{\rm R}) \triangleq I_0 + I_1 = \sum_{i=0}^{1} P(d{=}i)\int_{-\infty}^{\infty} f(y_{\rm R}|d{=}i)\log\frac{f(y_{\rm R}|d{=}i)}{\sum_{k=0}^{1}P(d{=}k)f(y_{\rm R}|d{=}k)}{\rm d}y_{\rm R}, \tag{49}$$

where I_0 and I_1 correspond to the parts of $i = 0$ and $i = 1$, respectively.

Substituting (47) into I_0, we obtain that

$$I_0 = -p\log p - \frac{2p}{\sqrt{\pi\sigma_0^2}}\int_0^{\infty} {\rm e}^{-\frac{y_{\rm R}^2}{\sigma_0^2}}\log\left(1+\alpha{\rm e}^{-\beta y_{\rm R}^2}\right){\rm d}y_{\rm R}, \tag{50}$$

where $\alpha = \frac{1-p}{p}\sqrt{\frac{\sigma_0^2}{\sigma_1^2}}$ and $\beta = \frac{\sigma_0^2-\sigma_1^2}{\sigma_0^2\sigma_1^2}$.

The following lemma is provided below before we further compute I_0:

Lemma 2. For any $a, b, c > 0$, there is

$$\int_0^{\infty} {\rm e}^{-ay^2}\log\left(1+c{\rm e}^{-by^2}\right){\rm d}y = \frac{K^{-\frac{a}{b}}}{2\sqrt{b}}\sum_{k=1}^{K}\left(k-\frac{1}{2}\right)^{\frac{a}{b}-1}\left(\ln\frac{K}{k-\frac{1}{2}}\right)^{-\frac{1}{2}}\log\left(1+\frac{c(k-\frac{1}{2})}{K}\right). \tag{51}$$

Proof: Let $r = y^2$. Then we have ${\rm d}y = \frac{1}{2\sqrt{r}}{\rm d}r$ and

$$\int_0^{\infty} {\rm e}^{-ay^2}\log\left(1+c{\rm e}^{-by^2}\right){\rm d}y = \int_0^{\infty}\frac{{\rm e}^{-ar}}{2\sqrt{r}}\log\left(1+c{\rm e}^{-br}\right){\rm d}r. \tag{52}$$

Let $t = {\rm e}^{-br}$, i.e., $r = -\frac{\ln t}{b}$, ${\rm e}^{-ar} = t^{\frac{a}{b}}$ and ${\rm d}r = -\frac{1}{bt}{\rm d}t$. Then we have

$$\int_0^{\infty}\frac{{\rm e}^{-ar}}{2\sqrt{r}}\log\left(1+c{\rm e}^{-br}\right){\rm d}r = \frac{1}{2\sqrt{b}}\int_0^1 t^{\frac{a}{b}-1}\left(\ln\frac{1}{t}\right)^{-\frac{1}{2}}\log\left(1+ct\right){\rm d}t \triangleq \frac{1}{2\sqrt{b}}\int_0^1 f(t){\rm d}t. \tag{53}$$

A partition of an interval $[0, 1]$ is a finite sequence of numbers of the form $0 = x_0 < x_1 < x_2 < \cdots < x_n = 1$, while each $[x_i, x_{i+1}]$ is called a subinterval of the partition. The mesh or norm of a partition is defined to be the length of the longest subinterval, that is, $\max(x_{i+1} - x_i), i \in [0, n-1]$. A tagged partition $P(x, t)$ of the interval $[0, 1]$ is a partition together with a finite sequence of numbers $t_0, \cdots, t_{n-1}$, where t_i subject to the conditions that $t_i \in [x_i, x_{i+1}]$. In other words, it is a partition together with a distinguished point of every subinterval. The mesh of a tagged partition is the same as that of an ordinary partition.

The Riemann sum of $f(t)$ with respect to the tagged partition $x_0, \cdots, x_n$ together with $t_0, \cdots, t_{n-1}$ is given by [25]

$$\sum_{i=0}^{n} f(t_i)(x_{i+1} - x_i), \tag{54}$$

where each term in the sum is the product of the value of the function at a given point and the length of an interval. It is known that the Riemann integral is the limit of the Riemann sums of a function as the partitions get finer.

One popular restriction is the use of regular subdivisions of an interval. For example, the K-th regular subdivision of $[0,1]$ consists of the intervals as follows

$$\left[0,\frac{1}{K}\right],\left[\frac{1}{K},\frac{2}{K}\right],\cdots,\left[\frac{K-1}{K},1\right], \tag{55}$$

which divides $[0,1]$ into K subintervals with the k-th interval being $[\frac{k-1}{K},\frac{k}{K}]$, and picks out the midpoint of each interval as the tagged partitions, i.e., $t_k=\frac{k-\frac{1}{2}}{K}$. Since the Riemann sum can be made as close as desired to the Riemann integral by making the partition fine enough, K should be set relatively large.

Based on the above discussion, the integral in (53) can be computed as

$$\frac{1}{2\sqrt{b}}\int_0^1 f(t)\mathrm{d}t=\frac{1}{2\sqrt{b}}\sum_{k=1}^{K}\frac{1}{K}f(t_k)=\frac{1}{2K\sqrt{b}}\sum_{k=1}^{K}\left(\frac{k-\frac{1}{2}}{K}\right)^{\frac{a}{b}-1}\left(\ln\frac{K}{k-\frac{1}{2}}\right)^{-\frac{1}{2}}\log\left(1+\frac{c(k-\frac{1}{2})}{K}\right). \tag{56}$$

Thus Lemma 2 is proved. ■

According to Lemma 2, we can obtain the closed-form of I_0 as follows

$$I_0=-p\log p-pI_{00}, \tag{57}$$

where I_{00} is given by (58).

Similarly, the closed-form expression of I_1 can be derived as follows

$$\begin{aligned}I_1=&\frac{2(1-p)}{\sqrt{\pi\sigma_1^2}}\int_0^\infty \mathrm{e}^{-\frac{y_\mathrm{R}^2}{\sigma_1^2}}\left[\log\frac{\mathrm{e}^{-\frac{y_\mathrm{R}^2}{\sigma_1^2}}}{\sqrt{\sigma_1^2}}-\log\frac{p\mathrm{e}^{-\frac{y_\mathrm{R}^2}{\sigma_0^2}}}{\sqrt{\sigma_0^2}}-\log\left(1+\alpha\mathrm{e}^{-\beta y_\mathrm{R}^2}\right)\right]\mathrm{d}y_\mathrm{R}\\=&(1-p)\log\left(\frac{1}{p}\sqrt{\frac{\sigma_0^2}{\sigma_1^2}}\right)-\frac{(1-p)(\sigma_0^2-\sigma_1^2)}{2\sigma_0^2\ln 2}-(1-p)I_{11},\end{aligned} \tag{59}$$

where I_{11} is given by (60).

Combine (48), (50) and (59), we can obtain the following theorem:

Theorem 2. For the BISO channel of ambient backscatter, the mutual information between the input D and the output Y is

$$I(D;Y)=-2pI_{00}-2(1-p)I_{11}-2p\log p-2(1-p)\log\left(p\sqrt{\frac{\sigma_1^2}{\sigma_0^2}}\right)-\frac{(1-p)(\sigma_0^2-\sigma_1^2)}{\sigma_0^2\ln 2}. \tag{61}$$

Moreover, the capacity of the BISO channel can be expressed as

$$C_{\mathrm{BISO}}=\max_p I(D;Y). \tag{62}$$

Although it is difficult to derive the closed-form expression of the capacity of the BISO channel, we can simply apply a one-dimensional searching for the maximum $I(D;Y)$ since C_{BISO} is a function of one single variable p. We will obtain the capacity and the corresponding optimal input distribution via numerical simulation.

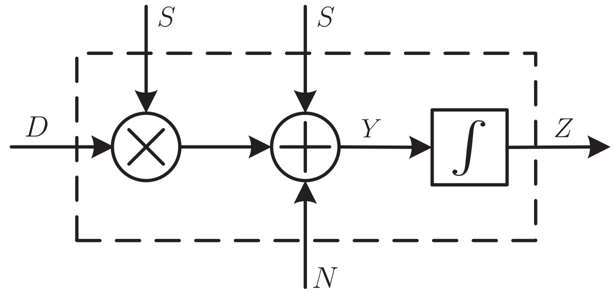

Fig. 4. Illustration of BIEO channel

V. Binary Input and Energy Output Channel

For theoretical interest, let us take the energy of the received signal at the reader as the continuous channel output, where the energy computator is treated as a part of the ambient backscatter channel. Since the output "energy" is an intermediate stage of the originally received signal and the binary bits after the threshold detection, one would expect that the information loss still exists compared to the BISO channel but is small compared to BIBO channel. Such a channel is named as the BIEO channel, as shown in Fig. 4.

Seen from Fig. 4, D, Y and Z constitute a Markov chain, i.e., $D\to Y\to Z$ [26], and they meet the relationship [27]:

$$p(d,z|y)=p(d|y)p(z|y). \tag{63}$$

Thus, the mutual information among them satisfy the following equation

$$I(D;Z|Y)=H(DZ|Y)-H(D|Y)-H(Z|Y)=0. \tag{64}$$

Moreover, with the equality $I(D;YZ)=I(D;Y)+I(D;Z|Y)=I(D;Z)+I(D;Y|Z)$, we have $I(D;Y)=I(D;Z)+I(D;Y|Z)$. Because of the non-negativity of the mutual information, there is $I(D;Y)\geq I(D;Z)$, which means that $I(D;Z)$ should be the lower bound of $I(D;Y)$.

In this section, we focus on the situation of $N=1$ for simplicity. It is known that the PDF of z for $N=1$ can be expressed as

$$f(z|d=i)=\frac{1}{\sigma_i^2}\mathrm{e}^{-\frac{z}{\sigma_i^2}}. \tag{65}$$

From (11), the mutual information of D and Z can be computed as

$$I(D;Z)\triangleq J_0+J_1=\sum_{i=0}^{1}P(d=i)\int_0^\infty f(z|d=i)\log\frac{f(z|d=i)}{\sum_{k=0}^{1}P(d=k)f(z|d=k)}\mathrm{d}z, \tag{66}$$

where J_0 and J_1 correspond to the parts of $i=0$ and $i=1$ in $I(D;Z)$, respectively.

Substituting (65) into part of $i=0$ in $I(D;Z)$, we have

$$\begin{aligned}J_0=&\frac{p}{\sigma_0^2}\int_0^\infty \mathrm{e}^{-\frac{z}{\sigma_0^2}}\left[-\log p-\log\left(1+\frac{(1-p)\sigma_0^2}{p\sigma_1^2}\mathrm{e}^{-\beta z}\right)\right]\mathrm{d}z\\=&-p\log p-\frac{p}{{\sigma_0}^2}\int_0^\infty \mathrm{e}^{-\frac{z}{\sigma_0^2}}\log\left(1+\frac{(1-p)\sigma_0^2}{p\sigma_1^2}\mathrm{e}^{-\beta z}\right)\mathrm{d}z.\end{aligned} \tag{67}$$

$$I_{00} = \sqrt{\frac{\sigma_1^2}{\pi(\sigma_0^2-\sigma_1^2)}} K^{\frac{-\sigma_1^2}{\sigma_0^2-\sigma_1^2}} \sum_{k=1}^{K} \left(k-\frac{1}{2}\right)^{\frac{2\sigma_1^2-\sigma_0^2}{\sigma_0^2-\sigma_1^2}} \left(\ln\frac{K}{k-\frac{1}{2}}\right)^{-\frac{1}{2}} \log\left(1+\frac{(1-p)\left(k-\frac{1}{2}\right)}{pK}\sqrt{\frac{\sigma_0^2}{\sigma_1^2}}\right). \tag{58}$$

$$I_{11} = \sqrt{\frac{\sigma_0^2}{\pi(\sigma_0^2-\sigma_1^2)}} K^{\frac{-\sigma_0^2}{\sigma_0^2-\sigma_1^2}} \sum_{k=1}^{K} \left(k-\frac{1}{2}\right)^{\frac{\sigma_1^2}{\sigma_0^2-\sigma_1^2}} \left(\ln\frac{K}{k-\frac{1}{2}}\right)^{-\frac{1}{2}} \log\left(1+\frac{(1-p)\left(k-\frac{1}{2}\right)\sqrt{\frac{\sigma_0^2}{\sigma_1^2}}}{pK}\right). \tag{60}$$

Before further deriving the closed-form expression of (71), we provide the following lemma:

Lemma 3. For any $a, b, c > 0$, there is

$$\begin{aligned}
&\int_0^{\infty} \mathrm{e}^{-az} \log\left(1+c\mathrm{e}^{-bz}\right) \mathrm{d}z \\
&= \frac{1}{bK^{\frac{a}{b}}} \sum_{k=1}^{K} \left(k-\frac{1}{2}\right)^{\frac{a}{b}-1} \log\left(1+\frac{c(k-\frac{1}{2})}{K}\right).
\end{aligned} \tag{68}$$

Proof: Letting $t = \mathrm{e}^{-bz}$, we have $\mathrm{e}^{-az} = t^{\frac{a}{b}}$ and $\mathrm{d}z = \frac{-1}{bt}\mathrm{d}t$, and it can be derived that

$$\begin{aligned}
\int_0^{\infty} \mathrm{e}^{-az} \log\left(1+c\mathrm{e}^{-bz}\right) \mathrm{d}z &= \frac{1}{b}\int_0^1 t^{\frac{a}{b}-1} \log(1+ct)\mathrm{d}t \\
&\triangleq \frac{1}{b}\int_0^1 g(t)\mathrm{d}t.
\end{aligned} \tag{69}$$

Similarly, we employ the K-th regular subdivision of $[0,1]$ which divides $[0,1]$ into K subintervals with the k-th interval being $[\frac{k-1}{K}, \frac{k}{K}]$, and pick out the midpoint of each interval as the tagged partitions, i.e., $t_k = \frac{k-\frac{1}{2}}{K}$.

Thus the Riemann Integral of (69) can be computed as

$$\begin{aligned}
&\frac{1}{b}\int_0^1 g(t)\mathrm{d}t = \frac{1}{b}\sum_{k=1}^{K}\frac{1}{K}g(t_k) \\
&= \frac{1}{b}\sum_{k=1}^{K}\frac{1}{K}\left(\frac{k-\frac{1}{2}}{K}\right)^{\frac{a}{b}-1} \log\left(1+\frac{c(k-\frac{1}{2})}{K}\right).
\end{aligned} \tag{70}$$

Lemma 3 is thus proved. ■

Based on Lemma 3, the closed-form expression of (71) can be expressed as

$$J_0 = -p\log p - pJ_{00}, \tag{71}$$

where J_{00} is given by (72).

Similarly, the part of $i = 1$ in $I(D;Z)$ can be derived as follows

$$\begin{aligned}
J_1 = (1-p)\int_0^{\infty} \frac{\mathrm{e}^{-\frac{z}{\sigma_1^2}}}{{\sigma_1}^2} &\left[\log\frac{\mathrm{e}^{-\frac{z}{\sigma_1^2}}}{\sigma_1^2} - \log\frac{p\mathrm{e}^{-\frac{z}{\sigma_0^2}}}{\sigma_0^2}\right. \\
&\left. - \log\left(1+\frac{(1-p)\sigma_0^2}{p\sigma_1^2}\mathrm{e}^{-\beta z}\right)\right] \mathrm{d}z \\
= (1-p)\log\left(\frac{\sigma_0^2}{p\sigma_1^2}\right) &- \frac{(1-p)(\sigma_0^2-\sigma_1^2)}{\sigma_0^2\ln 2} - (1-p)J_{11}.
\end{aligned} \tag{73}$$

where J_{11} is given by (74).

Combining (71) and (73), we can obtain the following theorem:

Theorem 3. For the BIEO channel of ambient backscatter, the mutual information between the input D and the output Z is

$$\begin{aligned}
I(D;Z) = &-pJ_{00} - (1-p)J_{11} - p\log p \\
&- (1-p)\log\left(\frac{p\sigma_1^2}{\sigma_0^2}\right) - \frac{(1-p)(\sigma_0^2-\sigma_1^2)}{\sigma_0^2\ln 2}.
\end{aligned} \tag{75}$$

Furthermore, the capacity of the BIEO channel can be expressed as

$$C_{\text{BIEO}} = \max_p I(D;Z). \tag{76}$$

Similarly, the closed-form expression of the capacity of the BIEO channel is hard to derive. However, since C_{BIEO} is a function of one single variable p, we can simply employ a one-dimensional search for the maximum $I(D;Z)$. We will display the capacity and the corresponding optimal input distribution via numerical simulation.

VI. Numerical Results

In this section, we resort to numerical simulation to evaluate the proposed studies. Compared with the distance between the source and the tag/reader, the distance between the tag and the reader is normally much shorter. We think that there might be a dominant line of sight between the tag and the reader, and Rician fading [28] may be more applicable for the channel between. Therefore, we generate the channels h_{sr}, h_{st} to follow $\mathcal{CN}(0,1)$ and make h_{tr} follow the normalized Rician distribution with the shape parameter $K = 10$ and the scale parameter $\Omega = 1$.

In the first example, we present the one-dimensional searching of $\frac{\partial C_{\text{BIBO}}(T_h)}{\partial T_h} = 0$ to numerically locate the optimal threshold T_h^* that maximizes $C_{\text{BIBO}}(T_h)$, and compare it with the ML detection threshold T_{ML} in Fig. 5. The BSC threshold T_{BSC} is also displayed for comparison. To facilitate demonstration, we take some different specific channel realizations while fix $N = 50$. As expected, it is seen that the optimal threshold T_h^* is an increasing function of SNR, since the gaps between σ_0^2 and σ_1^2 increases with SNR. Moreover, T_h^* is almost the same as T_{ML}, which allows us to use the closed-form T_{ML} for many other analytical or numerical studies. In addition, it is found that although the detection with T_{BSC}, i.e., equal detection error probability, cannot realize the optimal capacity, T_{BSC} is very close to T_h^*.

Fig. 6 shows the capacity of the BIBO channel (26) versus SNR for one specific realization of channel $h_{sr} = 0.26 - 1.40\mathrm{i}$, $h_{st} = -0.22 + 0.51\mathrm{i}$, and $h_{tr} = 0.89 + 0.19\mathrm{i}$, and the capacity ceiling (40) is also displayed for comparison. We set

$$J_{00} = \frac{\sigma_1^2 K^{\frac{-\sigma_1^2}{\sigma_0^2-\sigma_1^2}}}{\sigma_0^2-\sigma_1^2} \sum_{k=1}^{K} \left(k-\frac{1}{2}\right)^{\frac{2\sigma_1^2-\sigma_0^2}{\sigma_0^2-\sigma_1^2}} \log\left(1+\frac{(1-p)\sigma_0^2\left(k-\frac{1}{2}\right)}{p\sigma_1^2 K}\right). \tag{72}$$

$$J_{11} = \frac{\sigma_0^2 K^{\frac{-\sigma_0^2}{\sigma_0^2-\sigma_1^2}}}{\sigma_0^2-\sigma_1^2} \sum_{k=1}^{K} \left(k-\frac{1}{2}\right)^{\frac{\sigma_1^2}{\sigma_0^2-\sigma_1^2}} \log\left(1+\frac{(1-p)\sigma_0^2\left(k-\frac{1}{2}\right)}{p\sigma_1^2 K}\right). \tag{74}$$

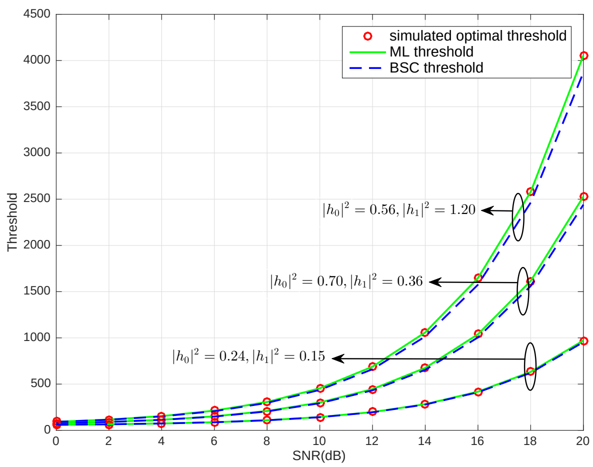

Fig. 5. Detection thresholds versus SNR for the BIBO channel of ambient backscatter under specific channel realization.

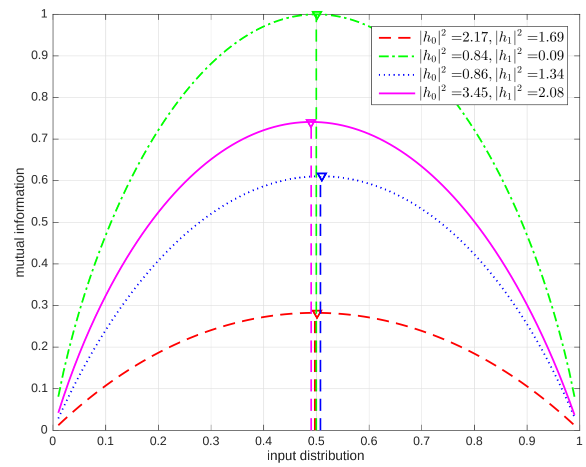

Fig. 7. Mutual information between the binary input D and the binary output $\hat{D}$ versus input distribution p for various channel realizations.

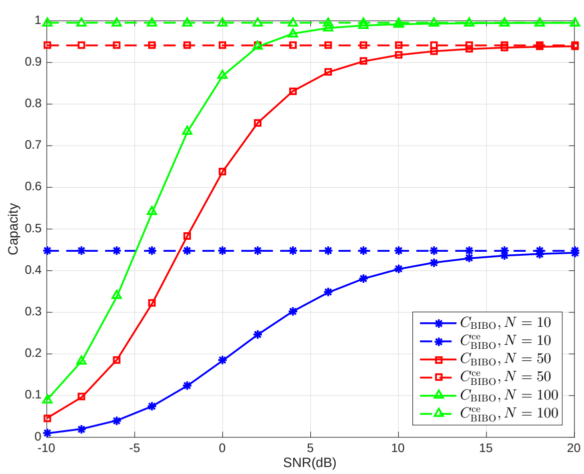

Fig. 6. Capacity of the BIBO channel versus SNR under a specific channel realization, where $h_{sr} = 0.26 - 1.40i$, $h_{st} = -0.22 + 0.51i$, and $h_{tr} = 0.89 + 0.19i$, and the detection threshold is set as $T_{\rm ML}$.

the detection threshold as $T_{\rm ML}$ and take $N = 10$, 50, and 100, respectively. It can be found that larger SNR leads to a higher capacity. However, when SNR becomes relatively large (say above 15 dB), the capacity will arrive at a ceiling which is consistent with the derived one (40). Interestingly, though our analysis is based on large N, it is seen that the capacity ceiling is also very accurate well when N is small.

We next show the mutual information between the binary input D and binary output $\hat{D}$ versus the input distribution p for various specific channel realizations in Fig. 7, where SNR = 10 dB, $N = 50$, and the detection threshold is set as $T_{\rm ML}$. The numerical maximum value of each mutual information curve is marked by a triangle, and the derived capacity-achieving input-distribution p^* (23) of each curve is marked by a dotted line. We see that the derived capacity-achieving input distributions matches the numerical results very well. It is also interesting to find that, for any channel value, the channel capacity is achieved almost by a uniform distribution on the input, i.e., $p = 0.5$. This is not unexpected since the optimal ML detection normally sets the optimal threshold in the middle of σ_0^2 and σ_1^2, i.e., the binary symmetrical channel, and hence, the inputs distribution should also be symmetric.

As we have shown in [7], [15], the relative channel difference (RCD) given by

$$\text{RCD} = \frac{||h_0|^2 - |h_1|^2|}{|h_0|^2 + |h_1|^2} = \frac{||h_{sr}|^2 - |h_{sr} + \alpha h_{st} h_{tr}|^2|}{|h_{sr}|^2 + |h_{sr} + \alpha h_{st} h_{tr}|^2} \tag{77}$$

makes a big difference in the detection performance. Thus, for random channel realization, we add a constraint that RCD ≥ 0.1 to avoid some poor channel conditions.

The mutual information between the binary input D and the signal output Y versus the input distribution p under random channel realization with RCD ≥ 0.1 is depicted in Fig. 8, where SNR = 10 dB and $N = 1$. Meanwhile, the partition number of the Riemann Integral, K, is set as 1000, 2000,

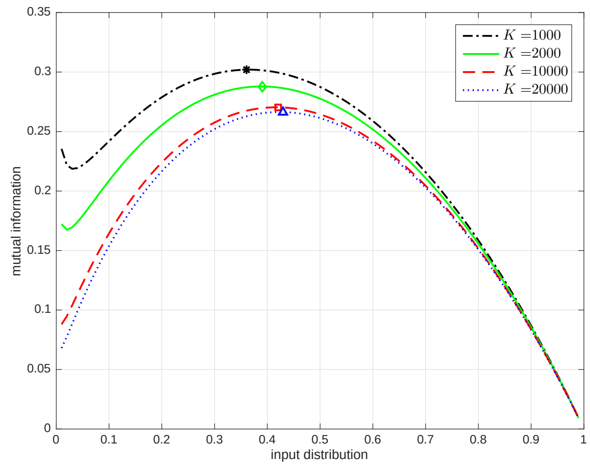

Fig. 8. Mutual information between the binary input D and the signal output Y versus input distribution under random channel realization with RCD ≥ 0.1.

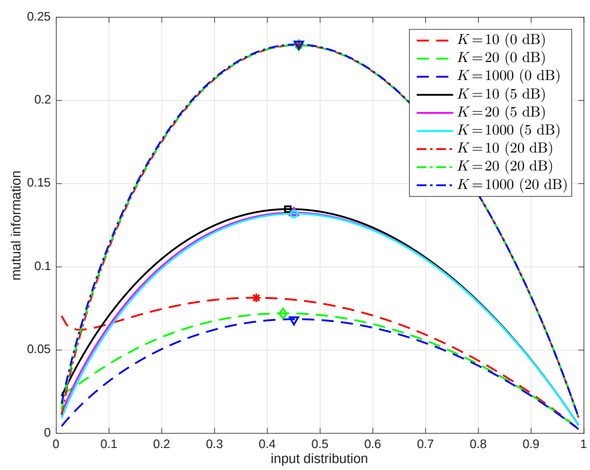

Fig. 9. Mutual information between the binary input D and the energy output Z versus input distribution under random channel realization with RCD ≥ 0.1.

10000 and 20000 for comparison. The numerical maximum value of each mutual information curve is marked by a spot. It can be found that when the partition number K is small, the derived mutual information (61) tends to distort at small input distribution. The larger the K is, the input distribution corresponding to the maximum mutual information will get closer to the uniform input distribution. However, the tendency will quickly descend as K increases.

We also demonstrate the mutual information between the binary input D and the energy output Z versus the input distribution p under random channel realization with RCD ≥ 0.1 in Fig. 9, where $N = 1$. Specifically, SNR is set to be 0 dB, 5 dB and 10 dB, and the partition number of the Riemann Integral K is set as 10, 20 and 1000 for comparison. The numerical maximum value of each mutual information curve is marked by a spot. It is shown that the larger the K is, the input distribution corresponding to the maximum mutual information will get closer to the uniform input distribution. However, when SNR is relatively large, the increase of K has little difference on the value of mutual information. Besides, compared with the BISO channel, the derived mutual information of the BIEO channel when K is small.

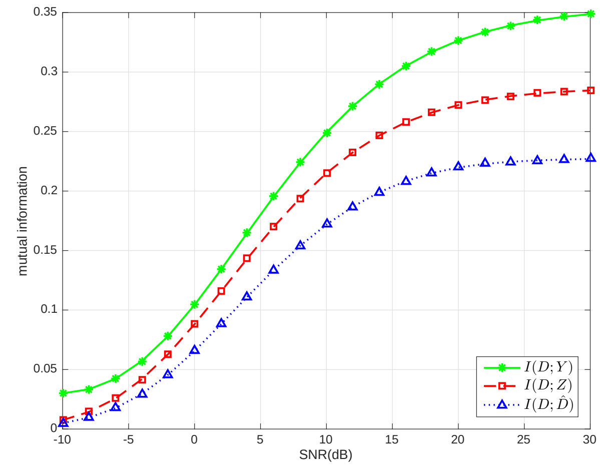

Fig. 10. Mutual information versus SNR for the three types of channel with RCD ≥ 0.2.

Lastly, we compare the mutual information between the binary input $\hat{D}$ and the binary output $\hat{D}$, the signal output Y, and the energy output Z, respectively, versus the SNR under random channel realization with RCD ≥ 0.2 in Fig. 10, where $N = 1$, $K = 10000$, and the binary input distribution is uniform. It is seen that $I(D;Y) \geq I(D;Z) \geq I(D;\hat{D})$, which can be verified since $D, Y, Z, \hat{D}$ form a Markov chain $Y \rightarrow Z \rightarrow \hat{D}$.[3] In addition, the larger the SNR is, the larger the mutual information will be. The mutual information of the three kinds of channels will approach a ceiling level when the SNR grows to a certain value, say 20 dB.

VII. Conclusion

In this paper, we investigate three kinds of channels, i.e., the BIBO, BISO and BIEO channels, for the ambient backscatter system from information theoretic viewpoint. For the BIBO channel, we derived the closed-form expressions of the mutual information, the capacity, the capacity-achieving input distribution, and a tight capacity ceiling when SNR turns relatively large. For the BISO and BIEO channels, we computed the closed-form mutual information between their inputs and outputs, respectively, while their semi-closed-form capacity values can be obtained from one dimensional searching. Simulation results show that the threshold maximizing the BIBO capacity is almost the same as that of the ML detector. Moreover, the mutual information of the BIEO channel is the lower bound of that of the BIBO channel, but is the upper bound of that the BISO channel. In addition, the capacity of all three different channels are achieved almost by the uniform input distribution.

[3] Intuitively, signal processing can cause information loss.

REFERENCES

[1] L. Yan, Y. Zhang, L. T. Yang, and H. Ning, *The Internet of Things: From RFID to the next-generation pervasive networked systems*. Boca Raton, FL, USA: Auerbach Publications, 2008.

[2] H. Jayakumar, K. Lee, W. S Lee, and A. Raha, "Powering the Internet of Things," in *ISLPED'14*, La Jolla, CA, USA, Aug. 2014, pp. 375-380.

[3] V. Liu, A. Parks, V. Talla, S. Gollakota, D. Wetherall, and J. R. Smith, "Ambient backscatter: wireless communication out of thin air," in *Proc. ACM SIGCOMM'13*, Hong Kong, China, Aug. 2013, pp. 39–50.

[4] A. Parks, A. Liu, S. Gollakota, and J. R. Smith, "Turbocharging ambient backscatter communication," in *Proc. ACM SIGCOMM'14*, Chicago, Illinois, USA, Aug. 2014, pp. 619–630.

[5] C. Boyer and S. Roy, "Backscatter communication and RFID: coding, energy, and MIMO analysis," *IEEE Trans. Commun.*, vol. 62, no. 3, pp. 770–785, Mar. 2014.

[6] G. Wang, F. Gao, R. Fan, and C. Tellambura, "Ambient backscatter communication systems: detection and performance analysis," *IEEE Trans. Commun.*, vol. 64, no. 11, pp. 4836–4846, Nov. 2016.

[7] J. Qian, F. Gao, G. Wang, S. Jin, and H. Zhu, "Noncoherent detections for ambient backscatter system," *IEEE Trans. Wireless Commun.*, vol. 16, no. 3, pp. 1412–1422, Mar. 2017.

[8] J. Qian, F. Gao, and G. Wang, "Signal detection of ambient backscatter system with differential modulation," in *Proc. IEEE ICASSP'16*, Shanghai, China, Mar. 2016, pp. 3831–3835.

[9] G. Yang, Y. Liang, R. Zhang, and Y. Pei, "Modulation in the air: Backscatter communication over ambient OFDM carrier," *IEEE Trans. Commun.*, vol. 66, no. 3, pp. 1219–1233.

[10] G. Yang, Q. Zhang, and Y. Liang, "Cooperative ambient backscatter communications for green Internet-of-Things," *IEEE Internet things J.*, vol. 5, no. 2, pp. 1116–1130, Apr. 2018.

[11] D. T. Hoang, D. Niyato, P. Wang, D. I. Kim, and Z. Han, "Ambient backscatter: A new approach to improve network performance for RF-powered cognitive radio networks," *IEEE Trans. Commun.*, vol. 65, no. 9, pp. 3659–3674, Sep. 2017.

[12] Q. Tao, C. Zhong, H. Lin, and Z. Zhang, "Symbol detection of ambient backscatter systems with Manchester coding," *IEEE Trans. Wireless Commun.*, vol. 17, no. 6, pp. 4028–4038, Jun. 2018.

[13] D. Darsena,G. Gelli and F. Verde, "Modeling and performance analysis of wireless networks with ambient backscatter devices," *IEEE Trans. Commun.*, vol. 65, no. 4, pp. 1797–1814, Apr. 2017.

[14] J. Qian, F. Gao, S. Jin, L. Xing, and J. Zhao, "Capacity of Ambien Backscatter Communications with Binary Input and Binary Output Channel," in *Proc. IEEE GLOBECOM'18*, Abu Dhabi, UAE, Dec. 2018, pp. 1-5.

[15] J. Qian, F. Gao, G. Wang, S. Jin, and H. Zhu, "Semi-coherent detection and performance analysis for ambient backscatter system," *IEEE Trans. Commun.*, vol. 65, no. 12, pp. 5266-5279, Dec. 2017.

[16] E. Leitinger, B. C. Geiger, and K. Witrisal, "Capacity and capacity-achieving input distribution of the energy detector," in *IEEE International Conference on Ultra-Wideband*, Syracuse, NY, Sep. 2012, pp. 57–61.

[17] J. Singh, O. Dabeer, and U. Madhow, "On the limits of communication with low-precision analog-to-digital conversion at the receiver," *IEEE Trans. Commun.*, vol. 57, no. 12, pp. 3629–3639, Dec. 2009.

[18] J. Qian, F. Gao, G. Wang, and S. Jin, "Symbol detection and performance analysis of the ambient backscatter system," in *Proc. IEEE ICCC'16*, Chengdu, China, Jul. 2016, pp. 1–5.

[19] J. Qian, F. Gao, G. Wang, S. Jin, and H. Zhu, "Semi-coherent detector of ambient backscatter communication for the Internet of Things," in *Proc. IEEE SPAWC'17*, Hokkaido, Japan, Jun. 2017, pp. 898–902.

[20] I. S. Moskowitz, "Approximations for the capacity of binary input discrete memoryless channels," in *Proc. IEEE CISS10*, Princeton, NJ, USA, pp. 1-C5, Mar. 2010.

[21] Thomas M. Cover and Joy A. Thomas, *Elements of Information Theory*, New Jersy: Wiley-Interscience, 2nd edition, 2006.

[22] R. G. Gallager, *Information Theory and Reliable Communication*. New York: Wiley, 1968.

[23] R. Mathar and M. Dörpinghaus, "Threshold optimization for capacity-achieving discrete input one-bit output quantization," in *IEEE Int. Symp. on Inform. Theory*, Istanbul, Turkey, pp. 1999–2003, Jul. 2013.

[24] M. Abramowitz and I. A. Stegun, "Handbook of Mathematical Functions With Formulas, Graphs, and Mathematical Tables," New York: Dover, 1972.

[25] Steven G. Krantz, *Real Analysis and Foundations*, Boca Raton: CRC press, 4th edition, 2017.

[26] W. Zhao, G. Wang, F. Gao, Y. Zou, and S. Atapattu, "Channel capacity and lower bound for ambient backscatter communication systems," in *Proc. WCSP'17*, Nanjing, China, pp. 1–6, Oct. 2017.

[27] A. Papoulis and S. U. Pillai, *Probability, Random Variables and Stochastic Processes*, New York: McGraw-Hill, 4th edition, 2002.

[28] C. He and Z. J. Wang, "SER of orthogonal spaceCtime block codes over Rician and Nakagami-m RF backscattering channels," *IEEE Trans. Veh. Technol.*, vol. 63, no. 2, pp. 654–663, Feb. 2014.

Jing Qian received the B.Eng. degree in communication engineering from Nanjing University of Science and Technology, Nanjing, China, in 2013, and the Ph.D. degree in the Department of Automation from Tsinghua University, Beijing, China, in 2018. Her research interests include signal detection and performance analysis of backscatter communications.

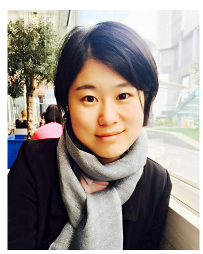

Yongxu Zhu (S'16, CM'19) received the M.S. degree from the Beijing University of Posts and Telecommunications, Beijing, China, and Dublin City University, Dublin, U.K., in 2012 and 2013, respectively, and the Ph.D. degree in electrical engineering from the University College London, London, U.K., in 2017. She is a Research Associate with the Loughborough University, Loughborough, U.K. Her research interests include UAV communications, wireless edge caching, millimeter-wave communications, heterogeneous cellular networks, and physical-layer security.

Chen He (M'14) received the B.Eng. degree (summa cum laude) from McMaster University in 2007, and the M.A.Sc. and Ph.D. degrees from The University of British Columbia (UBC), Vancouver, in 2009 and 2014, respectively, all in electrical and computer engineering. He was a Research Engineer at Blackberry Ltd., Canada, and a Post-Doctoral Research Fellow at UBC. He is currently a Full Professor with Northwest University, China. His research interests are the area of signal processing, wireless communications, and quantum information science.

Feifei Gao (M'09, SM'14) received the B.Eng. degree from Xi'an Jiaotong University, Xi'an, China in 2002, the M.Sc. degree from McMaster University, Hamilton, ON, Canada in 2004, and the Ph.D. degree from National University of Singapore, Singapore in 2007. He was a Research Fellow with the Institute for Infocomm Research (I2R), A*STAR, Singapore in 2008 and an Assistant Professor with the School of Engineering and Science, Jacobs University, Bremen, Germany from 2009 to 2010. In 2011, he joined the Department of Automation, Tsinghua University, Beijing, China, where he is currently an Associate Professor.

Prof. Gao's research areas include communication theory, signal processing for communications, array signal processing, and convex optimizations, with particular interests in MIMO techniques, multi-carrier communications, cooperative communication, and cognitive radio networks. He has authored/ coauthored more than 120 refereed IEEE journal papers and more than 120 IEEE conference proceeding papers, which have been cited more than 6500 times from Google Scholar.

Prof. Gao has served as an Editor of IEEE Transactions on Wireless Communications, IEEE Communcations Letters, IEEE Signal Processing Letters, IEEE Wireless Communications Letters, International Journal on Antennas and Propagations, and China Communications. He has also served as the symposium co-chair for 2015 IEEE Conference on Communications (ICC), 2014 IEEE Global Communications Conference (GLOBECOM), 2014 IEEE Vehicular Technology Conference Fall (VTC), as well as Technical Committee Members for many other IEEE conferences.

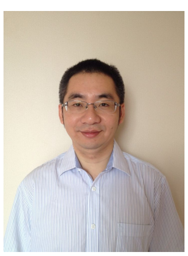

Shi Jin (S'06-M'07) received the B.S. degree in communications engineering from Guilin University of Electronic Technology, Guilin, China, in 1996, the M.S. degree from Nanjing University of Posts and Telecommunications, Nanjing, China, in 2003, and the Ph.D. degree in communications and information systems from the Southeast University, Nanjing, in 2007. From June 2007 to October 2009, he was a Research Fellow with the Adastral Park Research Campus, University College London, London, U.K. He is currently with the faculty of the National Mobile Communications Research Laboratory, Southeast University. His research interests include space time wireless communications, random matrix theory, and information theory. He serves as an Associate Editor for the IEEE Transactions on Wireless Communications, and IEEE Communications Letters, and IET Communications. Dr. Jin and his co-authors have been awarded the 2011 IEEE Communications Society Stephen O. Rice Prize Paper Award in the field of communication theory and a 2010 Young Author Best Paper Award by the IEEE Signal Processing Society.